Energy, Mines and Resources Canada

Énergie, Mines et Ressources Canada

CANMET

Canada Centre for Mineral and Energy Technology

Centre canadien de la technologie des minéraux et de l'énergie

Metals Technology Laboratories

Laboratoires de la technologie des métaux

Canada

Characteristic X-ray Mapping as an Aid to SEM Fractography

B.R. Casault, R.Dawson, W.N. Roberts,
M. Sahoo and M.T. Shehata

MTL 89-7 (TR)

This document is an unedited interim report prepared primarily for discussion and internal information purposes. It does not represent a final expression of the opinion of the Canada Centre for Mineral and Energy Technology (CANMET)

Ce document est un rapport provisoire non-révisé et rédigé principalement pour fin de discussion et de documentation interne. Il ne représente nullement l'expression définitive de l'opinion du Centre canadien de la technologie des minéraux et de l'énergie (CANMET)

MICROMEDIA

12 pp

CANMET

89-06220/

METALS TECHNOLOGY LABORATORIES
REPORT: MTL 89-7(TR)

CHARACTERISTIC X-RAY MAPPING AS AN AID TO SEM FRACTOGRAPHY

by

B.R. Casault*, R. Dawson** , W.N. Roberts*, M. Sahoo* and M.T. Shehata*

INTRODUCTION

In fractography, there is always a problem relating fractures on the fracture surface to the underlying structure. If conventional metallography is used, the fracture surface is destroyed in revealing the structure underneath, and correlations are difficult to make. We have shown that, under certain conditions, the location of second phase particles can be revealed by characteristic X-ray mapping without disturbing the fracture surface.

We have hypothesized that X-ray mapping to reveal structures of differing chemistry should be possible in a scanning electron microscope equipped with an X-ray energy dispersive analysis system (EDS), if the following criteria are met:

1. The alloy has distinct phases easily resolvable in the SEM.
2. The alloy shows strong partitioning of certain elements between the matrix and a second phase, assuming the elements are amenable to EDS.
3. The strongly partitioning elements are not too far apart in the periodic table. We rationalized that the probability of success would be enhanced if we could plot the ratio of the X-ray intensities of two partitioning elements point by point, rather than just their individual X-ray intensities, because the variation of intensity on a rough surface might well mask any chemical effects. In other words, ratio mapping could largely compensate for the variation of X-ray yield with X-ray emergence angle, particularly for two closely-spaced elements in the periodic table.

---

* Metals Technology Laboratories, Canada Centre for Mineral and Energy Technology, 568 Booth Street, Ottawa, Ontario, Canada K1A 0G1.

** Technical Manager, Deloro-Stellite Inc., 471 Dundas Street East, Belleville, Ontario, Canada K8N 5C4.

EXPERIMENTAL & RESULTS

The alloy chosen for analysis was commercial Stellite™ 6B which has essentially, with suitable hot-working, well spaced chromium carbide particles in a cobalt-rich matrix, as shown by an SEM backscattered/secondary electron micrograph of a conventional metallographic section (Fig. 1). This alloy has a nominal composition of 28 wt % Cr, 4 wt % W, 1.1 wt % C, 1.1 wt % Si and the balance Co. From Silence (1), an analysis of a 100 g sample of the 6B alloy would yield the following, for the principal alloying elements:

Weight (g/100 g of alloy)			
Solute	Alloy	Matrix	Carbide
Co	59.40	57.65	1.75
Cr	27.50	18.50	9.00
W	4.20	3.69	0.51
C	1.12	0.10	1.02

Weights of solutes in the matrix were obtained as the difference of weights in the alloy and the carbide phase. As a measure of partitioning, the Cr/Co atom ratio in the matrix is then

$$\frac{18.50}{52.01} \times \frac{58.94}{59.65} = 0.36$$

and in the carbide is

$$\frac{9.00}{52.01} \times \frac{58.94}{1.75} = 5.8$$

Chromium and cobalt were chosen for analysis because they are present in sufficient amounts to give a good X-ray signal, are sufficiently high in the periodic table that their characteristic X-rays are easily detectable with an Si (Li) detector and are close together in the periodic table with atomic numbers 24 and 27.

As a first step, we did X-ray mapping on the conventional metallographic section shown in Fig. 1, to minimise the complication of varying X-ray emergence angle. Figure 2 shows X-ray maps of (a) CrKα intensity, (b) CoKα intensity and (c) the ratio of CrKα to CoKα

™"Stellite" is a registered trademark of Stoody Deloro-Stellite Inc.

intensities smoothed. As will be discussed more fully later, the colours on the maps are quite arbitrary and have no particular significance other than being in the same order as the visible spectrum; the more the colour is toward the red end of the spectrum, the higher is the intensity, and the more it is toward the violet, the lower is the intensity. A close correlation is obvious between Fig. 1 and Fig. 2a, with the chromium intensity from the carbide particles being higher than from the matrix as expected. Likewise, there is a close correlation between Fig. 1 and Fig. 2b, with the cobalt intensity from the matrix being higher than from the carbide particles. Furthermore, Fig. 2c gives an even closer correlation between characteristic X-ray and backscattered/secondary electron intensity data, not unexpected because the Cr/Co ratio for the carbide is about 5.8 and for the matrix is about 0.36, a factor of about 16!

A fracture surface of Stellite™ 6B is shown in Fig. 3; areas which appear to be more cleaved than others are presumed to be cracked carbide particles. Figure 4a, the same field as Fig. 3, shows an area selected for EDS in the cleaved region; the corresponding characteristic X-ray spectrum is shown in Fig. 4b, which has a strong CrKα peak relative to the CoKα peak. Figure 5a, again the same field as Fig. 3, shows an area selected for EDS assumed to be in the matrix; the corresponding X-ray spectrum (Fig. 5b), as expected, shows a strong CoKα peak relative to the CrKα peak.

Characteristic X-ray intensity maps of the same area as Fig. 3 for CrKα, CoKα and CrKα/CoKα are shown in Fig. 6a, b and c. The cleaved areas of Fig. 3 are indeed shown (Fig. 6a) to be relatively high in chromium and low in cobalt, confirming that they are cracked carbide particles. The other areas are relatively low in chromium and high in cobalt (Fig. 6b), confirming that they are the matrix. The CrKα/CoKα map (Fig. 6c) appears to give the sharpest correlation with Fig. 3.

In some instances, the "X-ray area" of a mapped particle is larger than the area showing cleavage. We speculate that X-ray mapping will often show the projected area of a particle partially covered by matrix if X-ray absorption is not too strong.

Considerable manipulation of the X-ray data was needed to give clear maps. In the carbide, the CoKα signal often approached zero because of low counting statistics which gave very large Cr/Co ratios. We added a small integer to the intensity values in each pixel so that ratios would not tend to infinity. This artifice did not materially affect the ratios for mapping purposes. We also used various scaling factors to reproduce X-ray intensity data for the carbides and matrix in colours we found clear for reproduction purposes.

CONCLUSION

Characteristic X-ray mapping may be a valuable tool for correlating near surface structures based on chemical differences with features of the fractured surface of an alloy.

REFERENCES

1 Silence, W.L. "Effect of structure on wear resistance of Co-, Fe- and Ni-base alloys"; Wear of Materials, ASME; 1977.

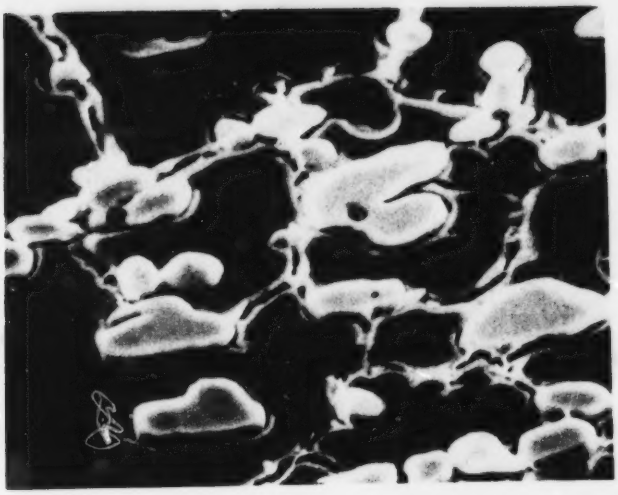

Fig. 1. SEM backscattered/secondary electron micrograph of a metallographic section of Stellite™ 6B alloy. (x3000)

Fig. 2a. CrKα map of the section in Fig. 1. (x3000)

Fig. 2b. CoKα map of the section in Fig. 1. (x3000)

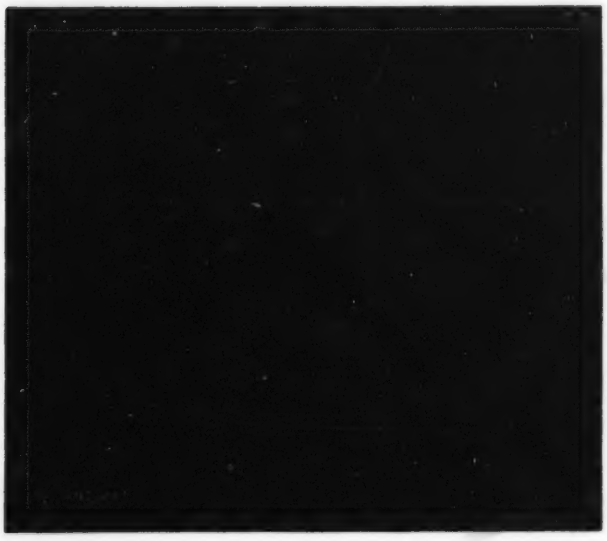

Fig. 2c. CrKα/CoKα map of the section in Fig. 1. (x3000)

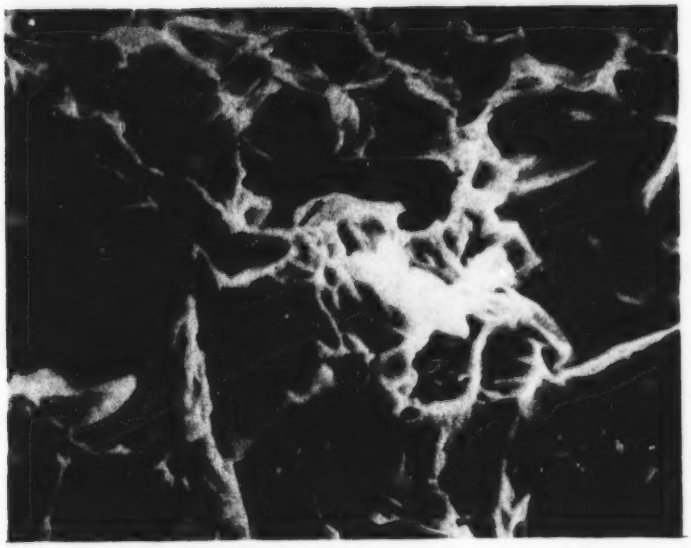

Fig. 3. Secondary electron micrograph of the fracture surface of Stellite™ 6B alloy. (x2500)

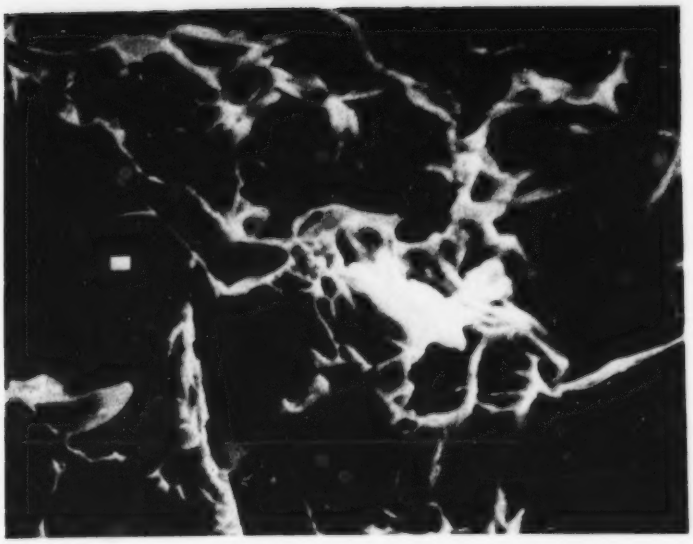

Fig. 4a. Same field as Fig. 3, showing area selected in a "carbide" for X-ray energy dispersive analysis. (x2500)

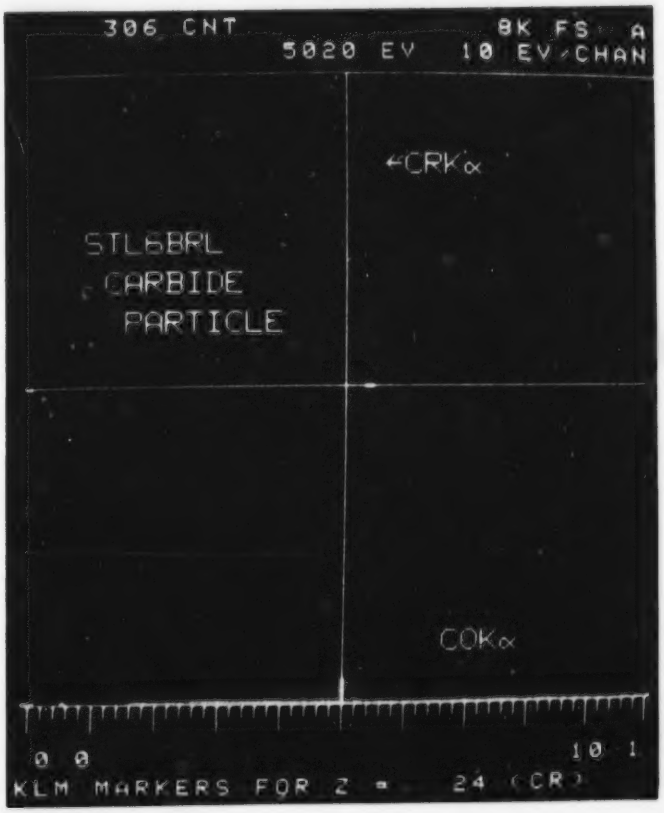

Fig. 4b. Characteristic X-ray spectrum of the area selected in Fig. 4a, showing a strong CrKα peak and weak CoKα peak.

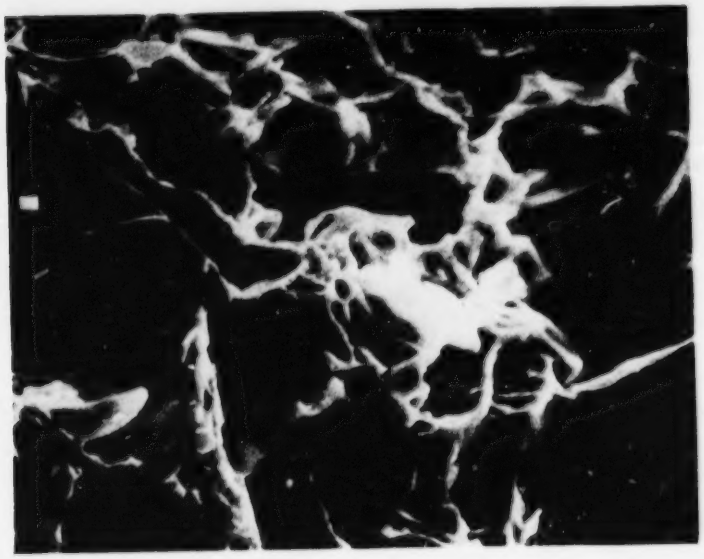

Fig. 5a. Same field as Fig. 3, showing area selected in the "matrix" for X-ray energy dispersive analysis. (x2500)

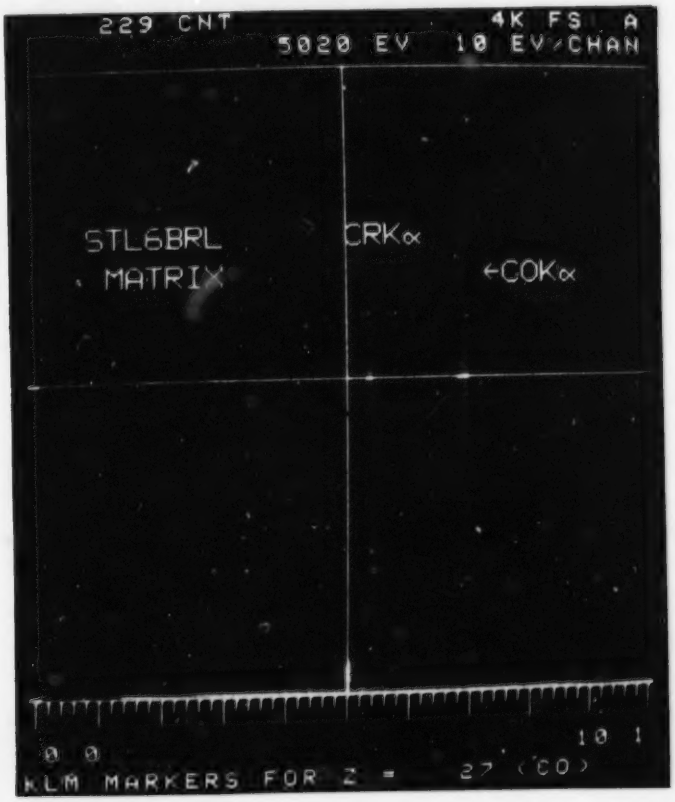

Fig. 5b. Characteristic X-ray spectrum of the area selected in Fig. 5a, showing a strong CoKα peak relative to the CrKα peak.

Fig. 6a. CrKα map of the fracture surface in Fig. 3. (x2500)

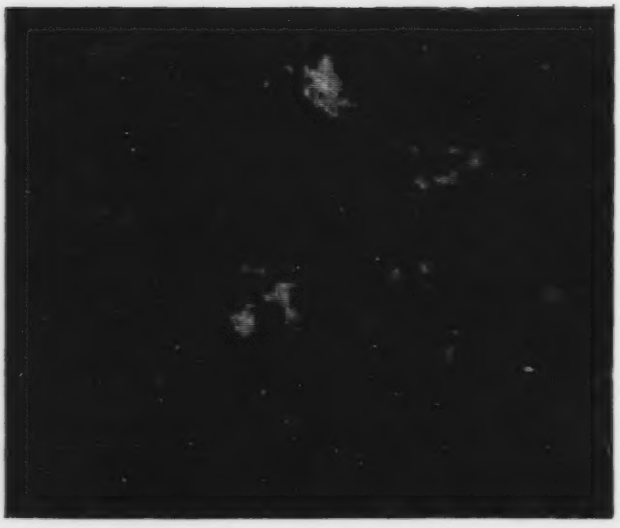

Fig. 6b. CoKα map of the fracture surface in Fig. 3. (x2500)

Fig. 6c. CrKα /CoKα map of the fracture surface in Fig. 3. (x2500)